*Article*

# Identification of groundwater sources in NO.1 Riverside Sliding Mass of Huangtupo Landslide using Environmental Stable Isotopes as Tracers

**Shen Cao [1], Xiangwei[1,2], Jinge Wang[2], Deshan Cui[1], Qingbing Liu[2]**

[1]  Faculty of Engineering, China University of Geosciences, Wuhan, 430074, China
[2]  Three Gorges Research Center for Geohazards, China University of Geosciences, Wuhan, 430074, China
*  Correspondence: xiangwei@cug.edu.cn

**Abstract:** Groundwater plays a crucial role in triggering and reactivating deep-seated landslides. However, classical hydrogeological investigations have limitations in their applicability to deep-seated landslides due to anisotropic and heterogeneous media. The Huangtupo landslide in the Three Gorges reservoir area has garnered significant attention in China due to its large volume, complex geological structure, and high hazard potential. Recent monitoring data has shown notable deformation in the NO.1 Riverside Sliding Mass (HTP-1), one of the four parts of the Huangtupo landslide, making it the primary focus of landslide research. This study aimed to investigate the water sources in the HTP-1 landslide using environmental stable isotopes as tracers. The isotopic analysis results indicated that the groundwater in the landslide area (LGW) is a mixture of remote karst groundwater (KGW) from the adjacent up-slope and local precipitation (LP). The karst groundwater is a major contributor to the recharge of the landslide groundwater system, causing a high slope groundwater level that can easily exceed the critical level during heavy rainfall events. Furthermore, based on the differential distribution of the LP fraction of LGW at different locations, the groundwater in the landslide can be classified into three groups. Groundwater at the sliding rupture surface has the highest fractions of local precipitation, followed by the groundwater at the rear of the landslide. Combined with the monitoring data of groundwater level in boreholes during the rainy season, this indicates that fissures and fractures in the sliding rupture zone and at the back of the landslide are well connected, which could be a critical factor in the mass movement of the creeping slope.

**Keywords:** Landslide; Slope groundwater source; Tracer; Environmental stable isotopes; Huangtupo; Three Gorges Reservoir

## 1. Introduction

Groundwater is known to play a significant role in the triggering and reactivation of deep-seated landslides. However, conventional hydrogeological investigations have limitations in their applicability to such landslides, which typically have anisotropic and heterogeneous media[1-4, 13, 18, 20]. The Huangtupo landslide in the Three Gorges reservoir area is one such landslide that has attracted considerable attention in China due to its large scale, complex geological structure, and high potential hazard. Of the four parts of the Huangtupo landslide, the NO.1 Riverside Sliding Mass (HTP-1) has shown notable deformation in recent monitoring data, making it the primary focus of landslide research (Fig. 1). Previous studies on the hydrogeology-related inferences of HTP-1 have mostly relied on planar geological surveys and monitoring of borehole water levels, and no targeted

research has been conducted to investigate the groundwater source in the landslide[7, 13, 19, 22, 23].
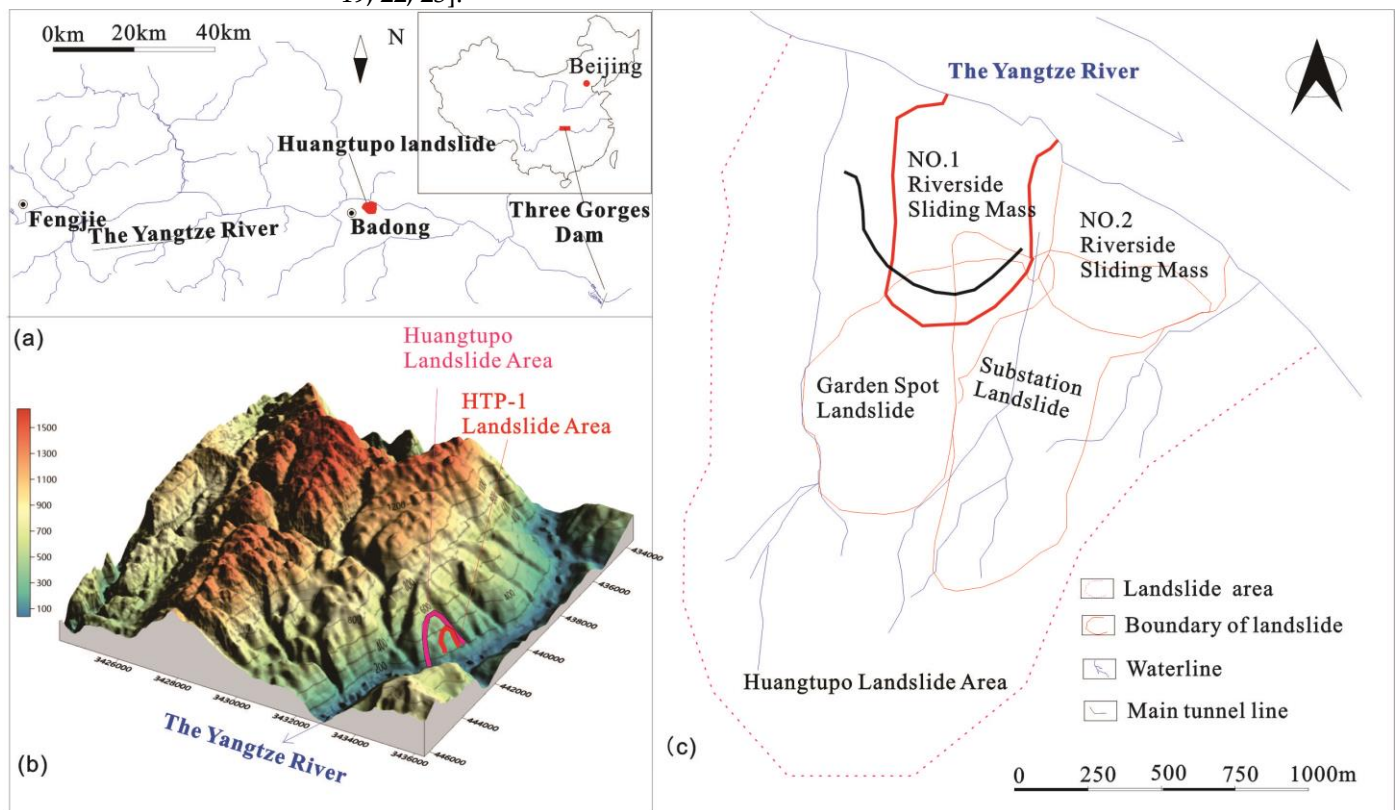


Figure 1 (a)The study area location in Yangtze River. Inset map shows the general location in China.

(b) 3D map of study area. (c) Distribution of four parts of the Huangtupo landslide and their respective locations

Previous studies have suggested that the groundwater source of the Huangtupo landslide is primarily from local precipitation based on its structural and lithological characteristics[12, 19]. Although karstic limestone containing groundwater is present at the top of the slope above the landslide, previous research suggested that the karstic water in the upper part of the slope could not replenish the groundwater in the landslide due to being isolated by the sandstone and mudstone layers of the Middle Triassic Badong Formation ($T_2b^2$), as well as the presence of the Badong Fault.

Instead, the karstic water was thought to flow through the limestone formations on both sides of the landslide and discharge into the Yangtze River, without replenishing the groundwater in the landslide.

Excavation of a 908-meter underground test tunnel in the rear part of the HTP-1 landslide in 2012 revealed that the groundwater system of the landslide consistently exhibited rapid and stable recharge characteristics. However, the recharge water, in terms of both volume and rate, cannot be solely attributed to local precipitation. Hydrochemical analysis of the groundwater of the landslide showed that it generally had high concentrations of sulfate ions (up to 120mg/L), while the primary lithology of the landslide is carbonate rock without detectable sulfate minerals. Based on these two points, it can be inferred that there is another stable and abundant recharge source for the landslide, in addition to local precipitation. Furthermore, this additional source of recharge water has caused a high groundwater level in the HTP-1, significantly increasing the risk of instability under rainfall conditions.

Hydrogen and oxygen stable isotopes are natural tracers of water bodies and are commonly used in the field of water resources investigation[1, 9, 16]. However, their application in the investigation and prevention of geological hazards is still in the explora-

tory stage[14, 15]. Specifically, investigations into the sources of groundwater in landslides are mostly limited to the landslide area[7, 8, 10, 13, 19, 21, 23], and there is a lack of large-scale groundwater sampling and analysis beyond the landslide boundary to identify the sources of groundwater in landslides using stable isotope information.

Isotope hydrogeochemistry theory holds that water from different sources has distinct hydrogen and oxygen stable isotope compositions, and that when the temperature is below 60°C, water-rock interaction has little impact on the hydrogen and oxygen stable isotope compositions of groundwater. As the groundwater temperature of the Huangtupo landslide remains below 28°C year-round, stable isotope tracing of hydrogen and oxygen proves to be an effective analytical method for investigating the groundwater sources.

In this study, the slope where the Huangtupo landslide is located was selected as the research area（Fig.2）, which includes the landslide area, the karst area above the landslide area, and the karst area on the east side of the landslide area. Comprehensive sampling and investigation of the research area was carried out to collect surface water, precipitation, and groundwater from different locations and depths. The primary method used was hydrogen and oxygen stable isotope analysis, supplemented with regional geological survey reports and isotope data of nearby precipitation for analysis, to reveal the sources of groundwater in the Huangtupo landslide.

## 2. Materials and Methods

### 2.1 Study area

The study area is located in the Three Gorges Reservoir Area of Badong County, Hubei Province, China (Fig.1a). The area has distinct seasons, abundant rainfall, with an annual average rainfall of 1100.7mm, mainly concentrated from April to September, accounting for 71.8% of the total annual rainfall. The Huangtupo landslide is located on the fan-shaped slope on the south bank of the Yangtze River (Fig.1b), with an area of $135 \times 104 m^2$ and a volume of $6934 \times 104 m^3$. The sliding surface is approximately 50-100m deep and comprises both structurally loose fragmented rocks and block rocks, as well as multiple layers of soft interbedded clay with high content. The main exposed strata in the study area are the 1-3 sections of the Middle Triassic Badong Formation ($T_2b^1$, $T_2b^2$, $T_2b^3$) and the Lower Triassic Jialingjiang Formation (Fig.2a). The main lithologies include the muddy limestone, dolomite, and mudstone of the first and third sections of the Badong Formation, the interbedded sandstone and mudstone of the second section of the Badong Formation ($T_2b^2$), and the limestone, dolomite, gypsum pseudomorph micritic limestone, gypsum-cemented dolomite of the third section of the Jialingjiang Formation ($T_1j^3$) 。

The NO.1 Riverside Sliding Mass (HTP-1) is one of the four parts of the Huangtupo landslide, situated in the Three Gorges Reservoir area in Hubei Province, China. Given its direct contact with the Yangtze River and the periodic fluctuations of the reservoir water level (ranging from 145 m to 175 m), HTP-1 landslide is the main and most dangerous area of the landslide, making it the primary focus of landslide research (Fig.1c).

To this end, the Three Gorges Research Center for Geohazards (TGRC) of the China University of Geosciences (CUG), supported by the China Ministry of Education, built a large field test site in the Huangtupo landslide to provide an unprecedented opportunity to research reservoir landslides (Fig.1c). A group of tunnels with a total length of 1.1 km has been constructed in the HTP-1 landslide, Additionally, nine boreholes, with a cumulative length of 894 m, have been drilled into the sliding mass[22]. The main tunnel traverses the sliding bed, sliding zone, and sliding mass of the landslide from west to east, (Fig. 2b). The third and fifth branch tunnels (BR3、BR5) were excavated from south to north to expose the sliding zone. This experimental site provides excellent conditions for sampling groundwater, particularly fresh groundwater near the sliding rupture zone, at various locations within the landslide.
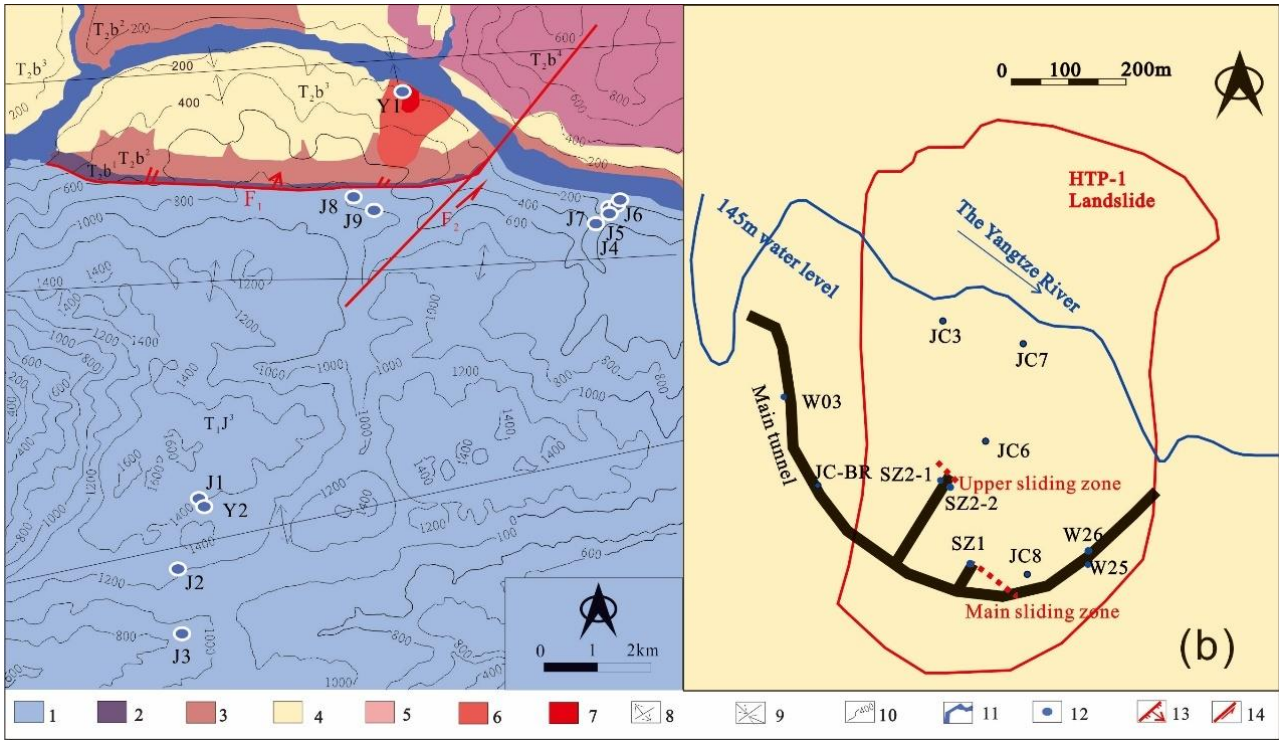
Figure 2 (a) Geological sketch map of study area. *Legend: 1. $T_1j^3$；2.$T_2b^1$；3$T_2b^2$；4. $T_2b^3$；5. $T_2b^4$；6.Huang-tupo Landslide；7.HTP-1 Landslide；8. Anticline；9. Syncline；10. Contour line; 11. Water line；12. Sampling point；13. Badong fault；  14. Strike-fault*
（b）Engineering geological map and sampling locations of the HTP-1 landslide
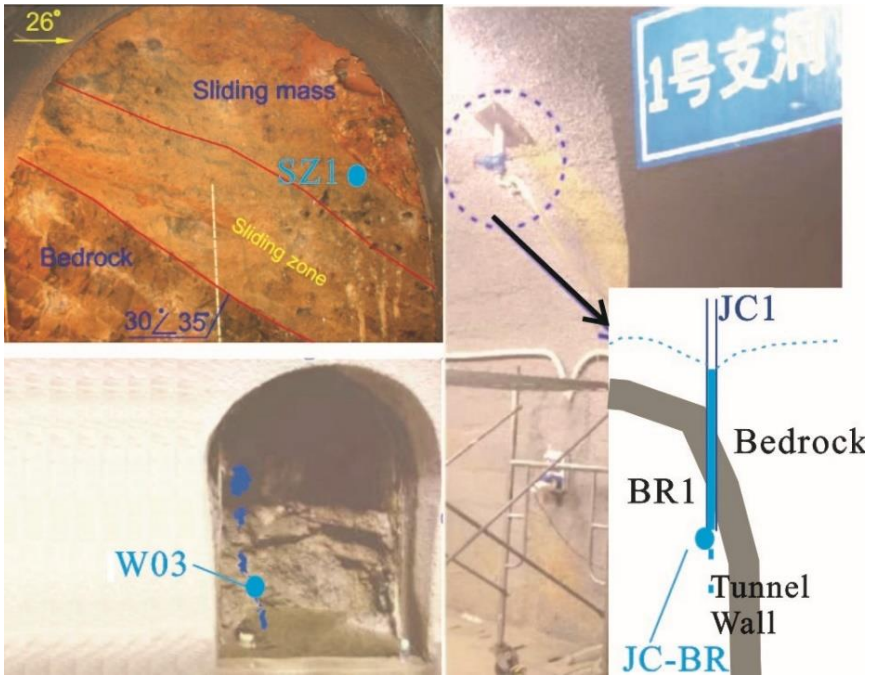


Figure 3 Photographs of sampling points in tunnels and their surrounding environment.

### 2.2 Samples

Clean polyester bottles were used for sample collection of precipitation, surface water, and groundwater in the study area, while the no-headspace sampling method was

employed to minimize the presence of bubbles in the samples. The bottles were thoroughly cleaned with distilled water prior to sampling and immediately filtered, sealed with wax, and stored at low temperatures after collection to reduce the influence of atmospheric hydrogen and oxygen on the groundwater samples during transportation and storage.

As the Huangtupo landslide is situated in the Three Gorges Reservoir area, the reservoir water level periodically fluctuates between 145-175 m, occasionally leading to brief supply of the slope groundwater with reservoir water when the water level is higher than the slope level. To minimize interference with the isotopic analysis of the groundwater samples, sampling was carried out in August during the low water level period (145.3 m) of the reservoir.

A total of 22 samples were collected in this sampling campaign, including 2 precipitation samples (Y1 and Y2), 9 samples from the karst area, and 11 samples from the landslide area. Among the samples from the karst area, J8 and J9 were surface water samples, and the rest were groundwater samples from different elevations. It should be noted that among the 11 water samples in the landslide area, JC3, JC7, JC6, JC8 were obtained from the boreholes, W03, W25, W26 from the groundwater exposure point reserved on the side wall of the underground tunnel, SZ1, SZ2-1, SZ2-2 from the tunnel faces which expose the sliding zone, and BR-JC from the bottom of the drainage borehole JC1 and the top of the tunnel BR1 (Fig.3). The drainage borehole JC1 was drilled downwards from the slope surface and intersects with the tunnel BR1, forming a three-dimensional drainage system that combines vertical boreholes and horizontal tunnels.

*2.3 Isotope analyses*

The collected samples were sent to the State Key Laboratory of Biogeology and Environmental Geology, China University of Geosciences (Wuhan) for analysis using an IWA-35-EP liquid water stable isotope analyzer from LGR(Los Gatos Research), USA. This instrument is based on the Beer Lambert law and the off-axis integrated cavity output spectroscopy (OA-ICOS) technology, which allows for simultaneous measurement of $\delta D$ and $\delta^{18}O$ compositions in water. The testing error for $\delta D$ is ±0.6‰ and for $\delta^{18}O$ is ±0.2‰. Before the samples were tested, they were filtered through a 0.22 μm syringe filter to remove any interference from particles in the water. The testing temperature was 26℃, and the final result for each tested sample and standard sample was the average of six measurements. The testing results are expressed in ‰ deviation values relative to V-SMOW (Vienna Standard Mean Ocean Water).

In order to ensure accurate and precise analysis of the water samples, the testing process was conducted in a state-of-the-art laboratory using advanced equipment and techniques. The IWA-35-EP liquid water stable isotope analyzer from LGR is a reliable and widely used instrument for water isotope analysis. By filtering the samples through a 0.22 μm syringe filter, we were able to eliminate any interference from particles and obtain more accurate results. The testing temperature was also closely monitored to ensure consistency and reliability of the results. The use of V-SMOW as a reference standard is widely accepted in the scientific community and provides a common basis for comparison of isotope data. Overall, these measures ensured that the results of the water isotope analysis were accurate, reliable, and scientifically valid.

## 3. Results and Discussion

### 3.1 LWML in study area

The isotopic composition of deuterium and oxygen in precipitation exhibits a linear relationship, known as the Meteoric Water Line (MWL). Rozanski et al. [17]conducted an analysis of 206 samples from the global AEA network stations and established the Global Meteoric Water Line (GMWL).   Similarly, Zheng et al. derived the MWL for China using 107 precipitation data. Due to the influence of local climate factors, such as the origin of water vapor, secondary evaporation during precipitation events, and seasonal variations in rainfall, local meteoric water lines differ among regions[5]. Therefore, this study employed the Yichang precipitation line equation located 63 km from Badong and the

Xiangxi River precipitation line equation situated 39 km from Badong as auxiliary analyses[11]. Measured precipitation data is presented in Table 2, and the measured data and multiple precipitation lines are plotted in Fig. 4. Results demonstrate that the stable isotopic composition of precipitation in the study area is highly consistent with the precipitation line equations of Yichang and Badong. Thus, the Xiangxi River precipitation line, which is closer to Badong, was selected as the Local Water Meteoric Line (LWML) expressed as:

$$\delta D = 8.17\ \delta^{18}O + 13.38; \qquad (1)$$

$$N = 92\ R = 0.995.$$

### 3.2 Altitude effect of precipitation in study area

Different positions of precipitation exhibit a decrease in δD and δ18O values with increasing terrain elevation, which is referred to as the altitude effect and typically exhibits a linear relationship [14]. Stable isotope values in high-elevation regions are generally relatively lighter than those in low-elevation regions. This altitude effect is commonly applied to analyze the recharge elevation of groundwater. In this study, the altitude gradient was calculated to be -0.26‰/100m based on two rainwater samples. However, because of the limited number of rainwater samples, directly using this altitude gradient as the local precipitation gradient lacks support. Huang et al. (2015) conducted a year-long hydrological monitoring of precipitation in the Xiangxi River basin[11], located 39 km from Badong, and obtained a δ18O altitude gradient of -0.26‰/100m based on isotopic data from 92 samples. Furthermore, Yu (1980) [24, 25]investigated the altitude effect of stable isotope compositions in precipitation in the Sichuan, Guizhou, and Tibet regions of China and obtained a δ18O altitude gradient of -0.26‰/100m. The consistency of this calculated value with the reference value from the literature supports the applicability of this altitude gradient in this study. The mathematical regression between δ18O value and altitude can be expressed as follows:

$$\delta^{18}O = -2.6 \times 10^{-3}Z - 4.48 \qquad (2)$$

where δ18O represents the oxygen isotope composition of precipitation at a given elevation Z, and Z is in meters (EL).

**Table 1.** Stable oxygen and hydrogen isotopic compositions for precipitation, surface water,　groundwater in karst area

| Samples | Y1 | Y2 | J1 | J2 | J3 | J4 | J5 | J6 | J7 | J8 | J9 |
|---|---|---|---|---|---|---|---|---|---|---|---|
| Elevation(m) | 276 | 1589 | 1500 | 1249 | 905 | 301 | 285 | 192 | 219 | 812 | 815 |
| δD ‰ | −27. 5 | −56. 1 | -54.2 | -54.2 | -52.0 | -54.9 | -54.7 | -56.1 | -54.8 | -47.2 | -44.4 |
| δ18O ‰ | −5. 2 | −8. 6 | -8.5 | -8.5 | -8.3 | -8.5 | -8.6 | -8.5 | -8.6 | -6.1 | -6.0 |

**Table 2.** Stable oxygen and hydrogen isotopic compositions for groundwater in landslide area

| Samples | JC3 | JC7 | JC6 | JC8 | W26 | W25 | W03 | SZ1 | SZ2-1 | SZ2-2 | JC-BR |
|---|---|---|---|---|---|---|---|---|---|---|---|
| Z*/m | 142.0 | 143.0 | 162.8 | 195.6 | 190.0 | 190.0 | 180.0 | 185.0 | 185.0 | 185.0 | 180.0 |
| Z/m | 183.5 | 176.3 | 209.8 | 263.6 | 250.0 | 235.0 | 230.0 | 225.0 | 275.0 | 275.0 | 263.5 |
| δD ‰ | -53.0 | -54.4 | -53.4 | -50.1 | -52.1 | -53.0 | -54.4 | -49.1 | -46.2 | -44.7 | -49.0 |
| δ18O ‰ | -8.1 | -8.2 | -8.2 | -8.2 | -7.9 | -8.4 | -8.3 | -7.5 | -7.3 | -7.2 | -7.5 |

Z* represents the elevation of the sampling point

Z represents the corresponding slope surface elevation vertically above the sampling point.

### 3.3 Source of groundwater in study area

In this study, the relationship between δD and δ18O of each sample is shown in Fig. 5, and the regression line representing the local meteoric water line (LMWL) is δD = 8.17

δ¹⁸ O +13.38. It can be observed from Fig.5 that surface water (J8, J9) is influenced by evap-oration and exhibits varying degrees of isotopic enrichment, deviating from the LMWL. The isotopic data of groundwater in karst and landslide areas are distributed on the LMWL, indicating that the stable isotopes of these groundwater have not been signifi-cantly affected by water-rock interaction or evaporation. Therefore, the groundwater in the study area is not affected by surface water, and the local infiltration and underground transport of precipitation are the only causes of groundwater.
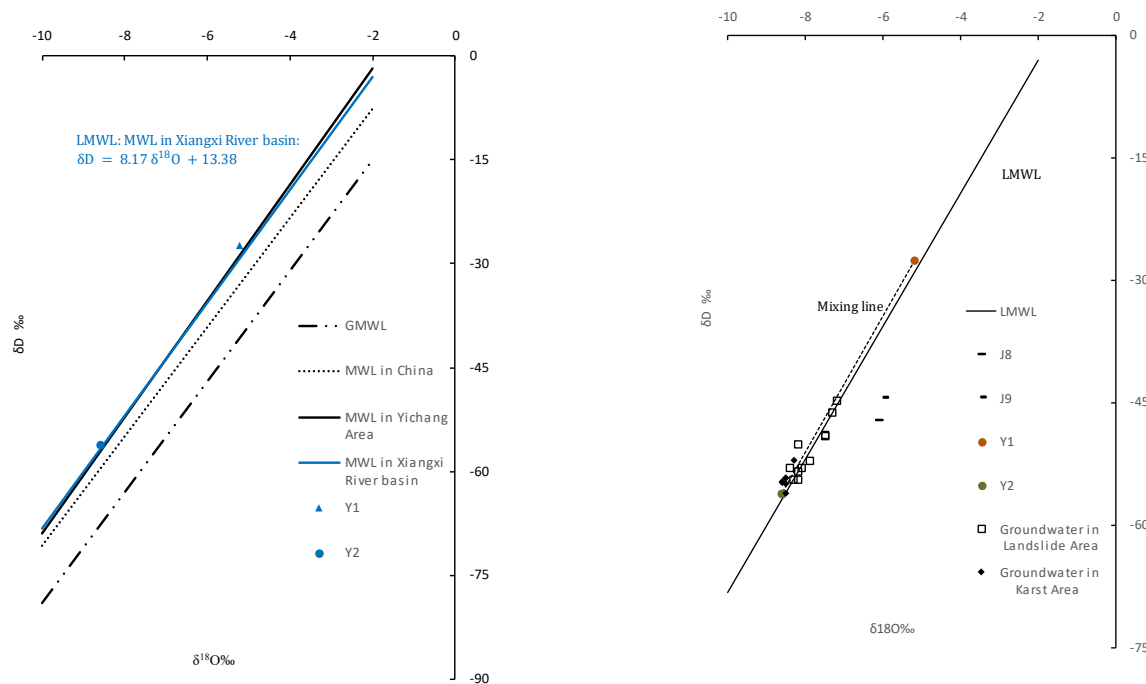


Figure 4.    Plot of  δD  versus  δ¹⁸O of measured precipitation. Meteoric water lines (WML) in global area, China Area, Yichang Area, Xiangxi Area.

Figure 5.    Plot of  δD  versus  δ¹⁸O of measured groundwater, surface water. Meteoric water lines in Xiangxi Area as LMWL.

3.3.1 Source of karst groundwater (KGW)

Seven groundwater samples in karst regions were collected at elevations ranging from 192 to 1500 meters. The stable isotope composition of $\delta^{18}O$  in these samples re-mained stable between -8.3‰ and -8.6‰. It is worth noting that the sampling sites of J4, J5, and J6 are located at the outlets of underground rivers deep in the karst riverside slope, where groundwater directly discharges into the Yangtze River. Sample J7 comes from a drainage hole in the deep mountainside along the Yangtze River. These four samples are all located in the discharge area of the karst groundwater system, and their stable isotope $\delta^{18}O$ values (-8.5‰ ~ -8.6‰) are still the same as the $\delta^{18}O$ value of the sample at the top of the slope at an elevation of 1500 meters(-8.5‰). Considering the measurement error range of the laser isotope analysis instrument of ±0.2‰, it can be assumed that the entire karst region has a relatively uniform recharge source. Based on formula (2), the theoretical ele-vation of the recharge area was calculated to be between 1489 and 1584 meters.

According to the regional tectonic background and geomorphic observation data, a second-level denudation surface (S2) with an elevation range of 1300-1500 meters exists in the study area, which is consistent with the calculated theoretical elevation range of the karst water supply area. The consistency of the calculated value with the objective geo-logical conditions further supports the applicability of formula (2) for estimating the water source in the study area.

3.3.2 source of landslide groundwater (LGW)

According to formula (2), the theoretical range of stable isotope δ¹⁸O values precipitation in the landslide area is calculated to be -4.5‰ to -5.2‰. The measured isotopic δ^18 O value of precipitation at 276 m elevation in the landslide area is -5.2‰, consistent with the theoretical range. However, the measured range of δ¹⁸O in the landslide groundwater is -7.2‰ to -8.4‰, much lower than the stable isotope content of local precipitation. This indicates that the landslide groundwater requires lighter δ¹⁸O sources from higher altitude precipitation to mix with the local precipitation. Furthermore, as discussed in the previous sections, surface runoff from the slope can be ruled out as a potential source. Therefore, it can be inferred that supplies from higher elevations can only enter the landslide groundwater system through subsurface flow.

Eleven LGW measured data points in the δ¹⁸ O -δD relationship graph are distributed on the mixing line of KGW (karst groundwater) measured data points and Y1 (precipitation on landslide) measured data points. Therefore, it is hypothesized that the landslide groundwater (LGW) is a mixture of nearby karst water (KGW) from the upper slope and local precipitation (LP) in the landslide area.

In the investigation report, it was found that the sulfate ion concentration in the landslide groundwater is high, with a maximum of 120 mg/L, while the main rock type in the landslide area is carbonate rock, and no sulfate rock or related minerals were detected. Considering that another potential source of the groundwater in the landslide area may be karst water from the upper mountain, the flow path of water transport must pass through the upper segment of the Jialingjiang Formation. Gypsum pseudomorph micritic limestone, gypsum-cemented dolomite is developed in this formation, and water-rock interactions during the runoff can explain the high sulfate ion concentration in the groundwater. This further confirms that one of the sources of the groundwater in the landslide area is the karst groundwater from the upper slope.

Estimating the relative contributions of karst water and local precipitation to the landslide groundwater can be achieved using a regular two-end member mass-balance equation[6, 15]. where X and (1-X) are the fractions of LP and KGW in LGW, respectively.

$$\delta^{18}O_{LGW} = X\,\delta^{18}O_{LP} + (1-X)\delta^{18}O_{KGW} \quad （3）$$

*3.4 The source fraction and significance of local precipitation*

Based on the Equation (3), the proportions of karst water and local precipitation in the groundwater of the landslide area were calculated and are presented in Table 3. The results show that the groundwater in the landslide area is mainly supplied by remote karst water from the adjacent up-slope, with proportions ranging from 58% to 92%. Meanwhile, the contribution of local precipitation to the groundwater in the landslide area is relatively small. Based on the differential distribution of the LP fraction of LGW at different locations, the groundwater in the landslide can be classified into three groups (as shown in Fig. 6).

In Group 1, the local precipitation fraction is observed to be the lowest, with both W03 and W25 LP fractions below 10%. W25 is sampled from the deep region of the sliding body at the front of the landslide, while W03 is sampled from the bedrock beneath the sliding bed at the rear. This indicates that there is no significant difference in the ability of sliding bed groundwater and sliding body groundwater to receive local precipitation. For large accumulative landslides such as HTP-1, multiple sliding events and long-term creep lead to the widespread development of weak interlayers within the sliding body. These interlayers consist mainly of silt clay or silt clay with crushed stones, which have an extremely low permeability coefficient and a random distribution, resulting in the deterioration of hydraulic properties and spatial anisotropy of the sliding body. Therefore, the study of hydraulic behavior of the HTP-1 landslide cannot simply rely on the sliding body-sliding zone-sliding bedrock structure as a basis, but should consider the actual groundwater flow in such slopes.

In Group 3, the contribution of precipitation to the landslide groundwater is relatively high (33%-42%). JC-BR was sampled at the intersection of drainage borehole JC1 and the horizontal drainage tunnel. The vertically distributed JC1 is located at the rear of

the landslide and can discharge the groundwater of the landslide downward, and then through the main tunnel that horizontally penetrates the landslide to discharge the land-slide. Due to its good hydraulic conductivity, it is inferred that the drainage channel has a strong ability to receive and collect local precipitation.

Table.3 Fractions of respective end sources contribute to groundwater in the studied landslide.

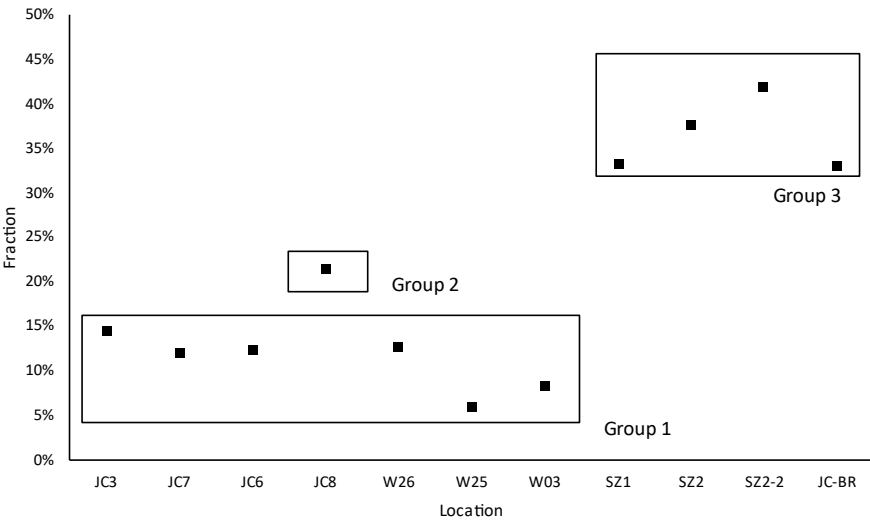| Samples | $\delta^{18}O$(‰) | Relative contributing fraction (%) |
|---|---|---|
| JC3 | -8.1 | $\delta^{18}O = 85\% \, \delta^{18}O_{KGW} + 15\% \, \delta^{18}O_{LP}$ |
| JC7 | -8.2 | $\delta^{18}O = 88\%\delta^{18}O_{KGW} + 12\% \, \delta^{18}O_{LP}$ |
| JC6 | -8.2 | $\delta^{18}O = 88\% \, \delta^{18}O_{KGW} + 12\% \, \delta^{18}O_{LP}$ |
| JC8 | -8.2 | $\delta^{18}O = 78\% \, \delta^{18}O_{KGW} + 22\% \, \delta^{18}O_{LP}$ |
| W26 | -7.9 | $\delta^{18}O = 87\%\delta^{18}O_{KGW} + 13\% \, \delta^{18}O_{LP}$ |
| W25 | -8.4 | $\delta^{18}O = 94\% \, \delta^{18}O_{KGW} + 6\% \, \delta^{18}O_{LP}$ |
| W03 | -8.3 | $\delta^{18}O = 92\% \, \delta^{18}O_{KGW} + 8\% \, \delta^{18}O_{LP}$ |
| SZ1 | -7.5 | $\delta^{18}O = 67\% \, \delta^{18}O_{KGW} + 33\% \, \delta^{18}O_{LP}$ |
| SZ2-1 | -7.3 | $\delta^{18}O = 62\% \, \delta^{18}O_{KGW} + 38\% \, \delta^{18}O_{LP}$ |
| SZ2-2 | -7.2 | $\delta^{18}O = 58\%\delta^{18}O_{KGW} + 42\% \, \delta^{18}O_{LP}$ |
| JC-BR | -7.5 | $\delta^{18}O = 67\%\delta^{18}O_{KGW} + 33\% \, \delta^{18}O_{LP}$ |



Fig.6 The source fractions of local precipitation on each landslide groundwater, respectively.

SZ2 and SZ1 were sampled from the upper sliding surface and the main sliding sur-face of the landslide, respectively. This suggests that the sliding rupture surface may pro-vide a continuous pathway for precipitation infiltration and runoff within the landslide. Thus, it can be inferred that preferential flow paths along the sliding rupture surface are the most developed.

Through analysis, it was found that the LP fraction in groundwater from sample JC8 fell between those of Group 1 and Group 3, second only to the LP fraction in groundwater from the sliding rupture surface and drainage system, and higher than the LP fraction in the other three boreholes. Borehole locations were JC6 (middle of the landslide), JC3 and

JC7 (front of the landslide), and JC8 (rear of the landslide), as depicted in Fig. 2. Groundwater level monitoring data from the four boreholes in Fig.7 showed that JC8 responded to precipitation significantly faster and to a greater extent than the other boreholes, which validated the analysis results of LP fraction in groundwater. These analytical results collectively indicate that the water-conducting pathway in the rear of the HTP-1 landslide is better developed, possibly due to more developed cracks and fissures in the rear caused by the movement of the landslide, and thus better connectivity. This finding has important implications for the stability analysis of large-scale slopes undergoing long-term creep and warrants further research and attention.
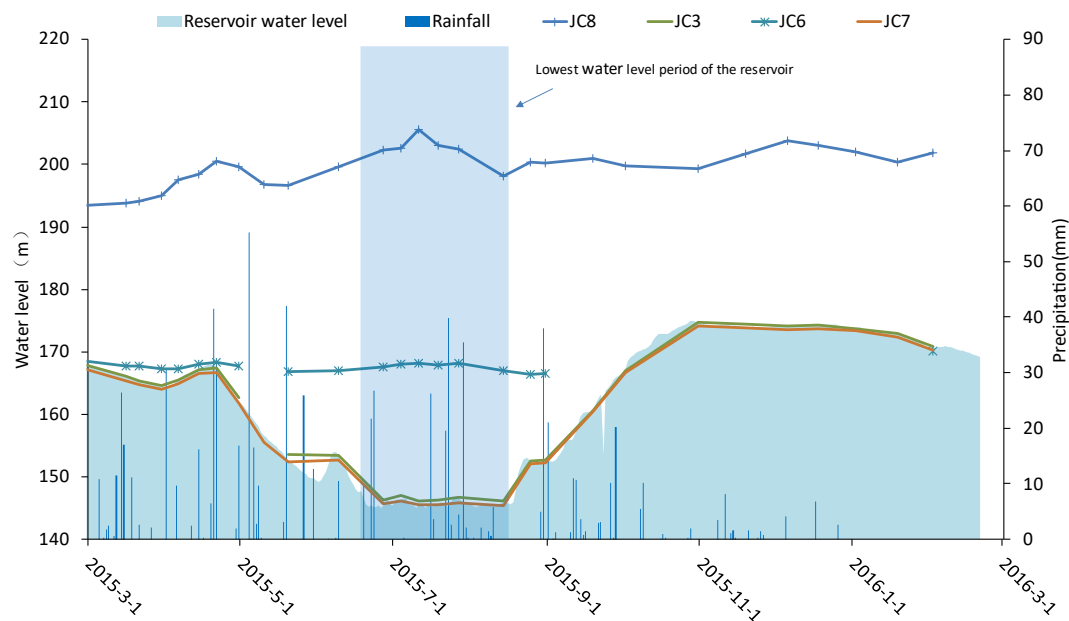


Fig.7 Continuous monitoring of groundwater levels for JC3, JC6, JC7, JC8, and reservoir water levels, as well as precipitation monitoring.

## 5. Conclusions

This study aims to investigate the water sources in the HTP-1 landslide using environmental stable isotopes as tracers. The isotope results show that the stable isotopic composition of precipitation in the study area is consistent with the precipitation line equations of Yichang and Xiangxi area and the local meteoric water line (LMWL) was established. The altitude gradient of $\delta^{18}$O in precipitation in the study area has been reliably estimated as -0.26‰/100m. The main source of karst groundwater (KGW) was estimated to be from the recharge area at an elevation of 1489-1584 meters. The source of landslide groundwater (LGW) was found to be a mixture of remote karst groundwater (KGW) from the adjacent up-slope and local precipitation (LP). The contribution of remote karst groundwater to the landslide groundwater was found to be relatively high, ranging from 58% to 92%, while the contribution of local precipitation was relatively small. Groundwater at the sliding rupture surface has the highest fraction of local precipitation, followed by the groundwater at the rear of the landslide. Combined with the monitoring data of groundwater level in boreholes during the rainy season, this indicates that fissures and fractures in the sliding rupture zone and at the back of the landslide are well connected, which could be a critical factor in the mass movement of the creep slope.

**Conflicts of Interest:** The authors declare no conflict of interest.

# References:

1. Bogaard, T., Guglielmi, Y., Marc, V., Emblanch, C., Bertrand, C. and Mudry, J. Hydrogeochemistry in landslide research: a review., *178* (2). 113-126.

2. Bogaard, T.A. and Greco, R. Preface:'Hillslope hydrological modelling for landslides prediction'.

3. Bogaard, T.A., Greco, R., Olivares, L. and Picarelli, L. The Round Robin Test on Landslide Hydrological Modeling at IWL2013. *Procedia Earth and Planetary Science*, *9*. 180-188.

4. Bogaard, T.A., Grecoa, R., Olivaresa, L. and Picarellia, L. The Round Robin test on landslide hydrological modeling at IWL2013.

5. Chern, X., Gan, Y., Liu, D., Li, X. and Yu, T. Spatial Distribution Characteristics of Hydrogen and Oxygen Isotopes in the Mainstream of Yangtze River. *Bulletin of Geological Science and Technology* (05). 110-114.

6. Criss, R., Fernandes, S. and Winston, W. Isotopic, Geochemical and Biological Tracing of the Source of an Impacted Karst Spring, Weldon Spring, Missouri. *Environmental Forensics*, *2* (1). 99-103.

7. Deng, Q.L., Zhu, Z.Y., Cui, Z.Q. and Wang, X.P. Mass rock creep and landsliding on the Huangtupo slope in the reservoir area of the Three Gorges Project, Yangtze River, China. *Engineering Geology*, *58* (1). 67-83.

8. Di Maio, C., Vassallo, R., Vallario, M., Pascale, S. and Sdao, F. Structure and kinematics of a landslide in a complex clayey formation of the Italian Southern Apennines. *Engineering Geology*, *116* (3-4). 311-322.

9. Gao, M., Li, X., Qian, J., Wang, Z., Hou, X., Fu, C., Ma, J., Zhang, C. and Li, J. Hydrogeochemical Characteristics and Evolution of Karst Groundwater in Heilongdong Spring Basin, Northern China. *Water*, *15* (4). 726.

10. Huang, F., Luo, X. and Liu, W. Stability Analysis of Hydrodynamic Pressure Landslides with Different Permeability Coefficients Affected by Reservoir Water Level Fluctuations and Rainstorms. *Water*, *9* (7). 450.

11. Huang, H., Luo, M., Chen, Z., Zhou, H. and Zhang, L. The spatial and temporal distribution of stable hydrogen and oxygen isotope of meteoric water in Xiangxi river basin. *Hydrogeology & Engineering Geology* (04). 36-42.

12. Huang, H., Song, D.S., Yun, H.S., Lee, D.H. and Cho, J.M. Water Level Change Caused from Three Gorges Dam Construction in Yangtze River Basin. *Journal of coastal research*, *SI* (64). 1672-1675.

13. Hua-xi, G. and Kun-long, Y. Study on spatial prediction and time forecast of landslide. *Natural Hazards*, *70* (3). 1735-1748.

14. Peng, T., Wang, C., Hsu, S., Wang, G., Su, T. and Lee, J. Identification of groundwater sources of a local-scale creep slope: Using environmental stable isotopes as tracers. *Journal of Hydrology*, *381* (1-2). 151-157.

15. Peng, T., Wang, C., Lai, T. and Ho, F.S. Using hydrogen, oxygen, and tritium isotopes to identify the hydrological factors contributing to landslides in a mountainous area, central Taiwan. *Environmental Geology*, *52* (8). 1617-1629.

16. Peters, E., Visser, A., Esser, B. and Moran, J. Tracers Reveal Recharge Elevations, Groundwater Flow Paths and Travel Times on Mount Shasta, California. *Water*, *10* (2). 97.

17. Rozanski, K., Araguás Araguás, L. and Gonfiantini, R. Isotopic patterns in modern global precipitation. *Climate change in continental isotopic records*. 1-36.

18. Shao, W., Bogaard, T.A., Bakker, M., Su, Y. and Berti, M. Analysing the influence of preferential flow on pressure transmission and landslide triggering. *Geophysical Research Abstracts, 17, EGU General Assembly, Vienna, Austria, 12-17 April 2015; EGU2015-7571*.

19. Tang, H., Li, C., Hu, X., Su, A., Wang, L., Wu, Y., Criss, R., Xiong, C. and Li, Y. Evolution characteristics of the Huangtupo landslide based on in situ tunneling and monitoring. *Landslides*, *12* (3). 511-521.

20.     Vallet, A., Charlier, J.B., Fabbri, O., Bertrand, C., Carry, N. and Mudry, J. Functioning and precipitation-displacement modelling of rainfall-induced deep-seated landslides subject to creep deformation. *Landslides*. 1-18.

21.     Van der Spek, J.E., Bogaard, T.A. and Bakker, M. Characterization of groundwater dynamics in landslides in varved clays. *Hydrology and Earth System Sciences, 17 (6), 2013*.

22.     Wang, J., Su, A., Xiang, W., Yeh, H., Xiong, C., Zou, Z., Zhong, C. and Liu, Q. New data and interpretations of the shallow and deep deformation of Huangtupo No. 1 riverside sliding mass during seasonal rainfall and water level fluctuation. *Landslides*, *13* (4). 795-804.

23.     Wu, S., Shi, L., Wang, R., Tan, C., Hu, D., Mei, Y. and Xu, R. Zonation of the landslide hazards in the forereservoir region of the Three Gorges Project on the Yangtze River. *Engineering Geology*, *59* (1－2). 51-58.

24.     Yu, J., Yu, F. and Liu, D. THE OXYGEN AND HYDROGEN ISOTOPIC COMPOSITIONS OF METEORIC WATERS IN THE EASTERN PART OF CHINA. *Geochimica* (01). 22-26.

25.     Yu, J., Zhang, H., Yu, F. and Liu, D. OXYGEN ISOTOPIC COMPOSITION OF METEORIC WATER IN THE EASTERN PART OF XIZANG. *Geochimica* (02). 113-121.